



ORIGINAL RESEARCH ARTICLE

Investigation on Microstructure, Hardness and Fracture Energy of AISI H13 Hot Work Tool Steel by Cyclic Heat Treatment

Ramin Meshkabadi, Vahid Pouyafar, and Reza Soltanikia

Submitted: 6 April 2023 / Revised: 31 May 2023 / Accepted: 11 June 2023 / Published online: 19 June 2023

This research aims to present the best conditions for cyclic heat treatment of AISI H13 hot work tool steel to improve its mechanical properties and achieve a microstructure with fine grains. To accomplish this, 27 experiments were designed using the full factorial design approach. The austenitizing, intermediate salt bath and quenching salt bath temperatures were kept constant, while the austenitizing times of 5, 10 and 15 min, holding in the intermediate bath of 5, 10 and 15 min and the number of cycles of 2, 3 and 4 were varied. The best mechanical properties were obtained with 5 min of austenitizing, 15 min of intermediate bath and 4 cycles, resulting in a 41% reduction in grain size and a significant increase in toughness compared to the control sample. EDX analysis revealed that higher austenitizing temperatures led to greater carbon dissolution in austenite, which in turn resulted in the formation of carbides and their penetration into grain boundaries, leading to grain boundary fracture.

Keywords AISI H13 hot work tool steel, cyclic heat treatment, fracture energy, hardness, microstructure

1. Introduction

Hot work tool steels are a popular choice for die components due to their impressive properties. These materials possess high levels of hot strength, making them resistant to deformation at high temperatures. They also have excellent tempering resistance, which allows them to maintain their hardness even after exposure to extreme heat. In addition, their ductility and low thermal expansion make them ideal for use in applications where dimensional stability is critical. Furthermore, hot work tool steels have high thermal conductivity, which allows them to efficiently transfer heat away from the die surface. Overall, these properties make hot work tool steels an excellent choice for die components in industrial settings (Ref 1-3).

All molds made of hot work tool steels must resist thermal shocks and have appropriate toughness and hardness. Hot work tool steels must deal with high-working temperatures, high loads during deformation, high-speed impact, abrasion, repetitive thermal and mechanical shocks, which shortens their life compared to cold work tool steels. Researchers use various techniques to improve their performance at high temperatures by increasing hardness, resistance to wear, corrosion and erosion. One of these methods is cyclic heat treatment by

controlling parameters such as temperature, austenitizing time and cooling time, which can change the steel structure and control the mechanical properties (Ref 4).

One of the widely used types of chromium hot work steel is AISI H13 that is commonly used in manufacturing and toolmaking. The elements present in H13 tool steel play a crucial role in determining its properties and performance. Chromium is the primary alloying element in H13 tool steel, which provides excellent resistance to wear and corrosion. Molybdenum and vanadium are also present in small amounts, which contribute to the steel's toughness and strength. Carbon is added to increase hardness and wear resistance, while silicon helps improve the steel's machinability and resistance to oxidation. Overall, the combination of these elements gives H13 tool steel excellent properties for use in high-temperature applications such as die casting, forging and extrusion (Ref 5). Heat treatment of these steels must be carried out in protected conditions such as vacuum furnaces and controlled environments due to decarburizing tendency. Inconsistencies in composition or uneven areas can sometimes arise during the manufacturing process of H13 tool steel, which can result in issues with its performance like premature wear or cracking. The process of homogenization and annealing involves subjecting steel to a controlled cycle of heating and cooling to eliminate any inconsistencies. The aim is to raise the temperature of the entire piece of steel to a uniform level and maintain it for a set duration, thus enabling any variations in composition to be leveled out (Ref 6).

The process of homogenization and annealing involves subjecting steel to a controlled cycle of heating and cooling to eliminate any inconsistencies. The aim is to raise the temperature of the entire piece of steel to a uniform level and maintain it for a set duration, thus enabling any variations in composition to be leveled out.

The mechanical properties of tool steels have been extensively studied over the years, particularly in relation to thermal

Ramin Meshkabadi, Faculty of Advanced Technologies, University of Mohaghegh Ardabili, Ardabil, Iran; and **Vahid Pouyafar** and **Reza Soltanikia**, Department of Manufacturing Engineering, University of Tabriz, Tabriz, Iran. Contact e-mail: r_meshkabadi@uma.ac.ir.

Table 1 Chemical composition of AISI H13 hot work tool steel

C	Si	Mn	P	S	Cr	Mo	V	Ni	Cu
0.38	1.12	0.46	0.022	0.009	5.08	1.27	0.97	0.25	0.11

Table 2 Process variables and their levels

Variable	Levels		
Austenitizing time (min)	5	10	15
Holding time in the intermediate bath (min)	5	10	15
Number of cycles	2	3	4

cycles and phase transformation. Research has shown that the microstructure and mechanical properties of AISI 1080 steel are influenced by the cooling rate during cyclic heat treatment, up to four cycles (Ref 7). Thermal cycling heat treatment has been found to increase the hardness and ultimate tensile strength of 13%Cr-4%Ni martensitic stainless steel, with a slight reduction in ductility (Ref 8). Fracture toughness is affected by both austenitizing and annealing temperatures, with H11 tool steel exhibiting the highest fracture toughness at an austenitizing temperature of 1020 °C followed by cooling (Ref 9). Meanwhile, a study on annealed medium-Mn steel evaluated the impact of austenitizing at two different temperature-time combinations on microstructural evolution and mechanical properties, revealing that the sample with a grain size of 20 μm exhibited superior strength and ductility compared to the sample with a grain size of 40 μm (Ref 10). Through the process of austempering, a bainitic steel with a low-carbon content was produced. This steel boasts an ultrahigh strength of approximately 1650 MPa, as well as an elongation and toughness of roughly 16% and 72 J/cm², respectively. The microstructure and mechanical properties of the steel were analyzed for different levels of prior austenite grain size. (Ref 11).

Studies have recently been carried out to investigate how various processes impact the mechanical characteristics of H13 steel and its composites. One such study by AlMangour et al. utilized the selective laser melting (SLM) technique to create a TiC-reinforced H13 steel composite with a finely heterogeneous structure. This structure exhibited greater hardness and elastic modulus compared to the unenhanced H13 steel, owing to the effects of grain refinement and strengthening (Ref 12). The impact of varying quenching and tempering temperatures on the microstructure and mechanical properties of H13 steel was examined by Wang et al. Their findings indicate that H13 steel displays a uniform microstructure with favorable strength and toughness when quenched at 1040 °C and tempered at 570 °C (Ref 13). Meanwhile, Ding et al. investigated ways to enhance the life of high pressure die casting (HPDC) dies made from H13 steel by examining the failure mechanisms. They found that erosion and cracking were the primary modes of failure, with fatal cracking frequently occurring around fillet radius due to elevated local stresses (Ref 14). Deirmina and colleagues utilized mechanical milling (MM) and SLM to create composites of AISI H13 steel reinforced with partially stabilized zirconia (PSZ). Their findings revealed that composite powders created through high-energy MM resulted in parts

with higher relative densities and microhardness compared to those created through low-energy MM. The tetragonal ZrO₂ formation highlighted PSZ's potential transformation toughening effect on fracture toughness (Ref 15). In a separate study, Li et al. improved the impact toughness and hardness of AISI H13 die steel by studying nitrogen addition's mechanism and changes in precipitate and microstructure (Ref 16).

Heat treatment is necessary in industry to obtain desired mechanical properties in a cost-effective manner. Cyclic heat treatment, including pre-treatment and repetitive quenching and tempering, is commonly used (Ref 7). A novel approach to cyclic heat treatment in a salt bath under A_{c1} temperature has been proposed to achieve an ultra-fine grain microstructure for H13 tool steel that is commonly used in forging, extrusion and die-casting industries. The steel's impact resistance is crucial for its use in forming industries (pressing and cutting molds and industrial mandrels at high temperatures), but consistency in microstructure during heat treatment has been a challenge. The objective of this study is to achieve a uniform and refined structure specially to produce large molds. The researchers propose a designed cyclic heat treatment to improve impact resistance and present the optimized process parameters for improved mechanical properties.

2. Materials and Methods

2.1 Preparation of Samples

AISI H13 hot work tool steel with chemical composition shown in Table 1 is used as starting material. Samples with cross-sectional dimensions of 10x10 mm and a length of 55 mm were prepared according to the ASTM E23 standard (Ref 17). All samples were mounted on a grinding machine using a magnetic clamp, and their surface was polished.

2.2 Experimental Details

In this study, two salt bath furnaces were used for cyclic heat treatment. The first and the second furnaces were set at a constant temperature of 1040 and 750 °C, respectively. Another salt bath furnace was used for hot quenching at 600 °C. The samples were then placed in furnaces with different cycles and holding times according to the designed experiments. The number of each cycle indicates the repetition of the cyclic heat treatment.

In this research, some heat treatment parameters are constant for all samples. These parameters are austenitizing at 1040 °C, intermediate salt bath at 750 °C and quenching at 600 °C. Variable parameters include austenitizing times of 5, 10 and 15 min, holding time in the intermediate bath of 5, 10 and 15 min and number of cycles 2, 3 and 4, according to Table 2. Samples preheated to 550 °C to prevent thermal shock. A laser thermometer monitored the temperature gradient and a digital timer monitored holding times.

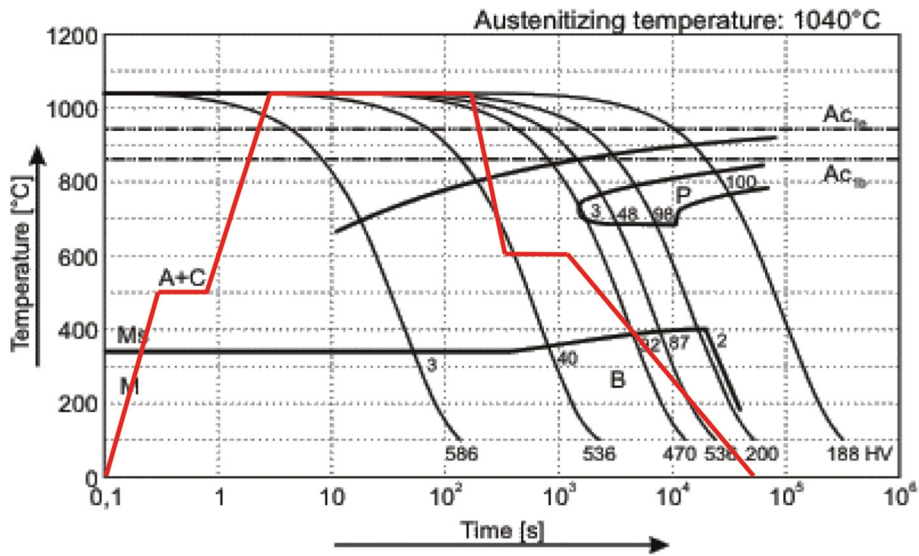


Fig. 1 The CCT diagram of H13 tool steel along with the used cycles

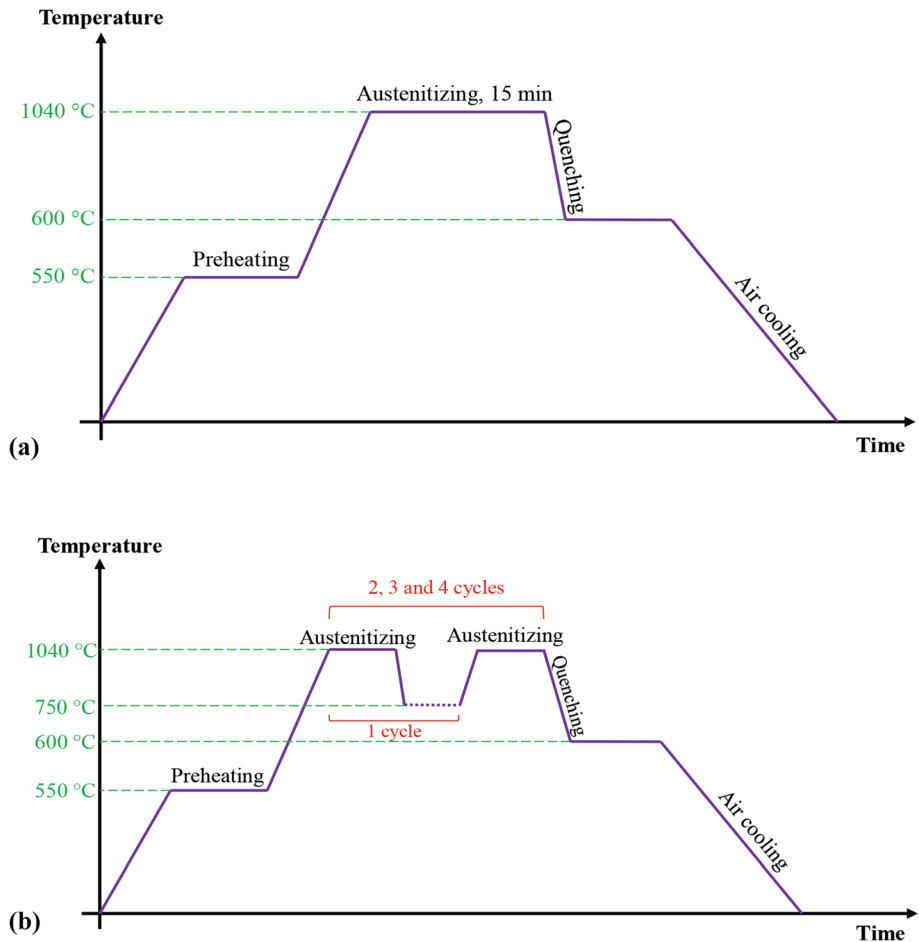


Fig. 2 Detailed cyclic heat treatment procedures: (a) first cycle (control sample) and 2, 3, (b) and 4 cycles

2.3 Cyclic Heat Treatment

The transformation temperatures of H13 tool steel depend on its composition and processing method. Austenite formation begins at around 820 °C (A_{c1} temperature) during heating,

while the entire structure transforms into austenite at approximately 940 °C (A_{c3} temperature). During cooling, the martensite start temperature (M_s) occurs around 340 °C. The microstructure and mechanical properties of H13 tool steel

Table 3 Designed experiments and obtained properties

Sample No.	Austenitizing time, min	Holding time in the intermediate bath, min	Number of cycles	Fracture energy, J	Hardness, RC	Grain size, μm
0	15	4	55.63	9.18
1	5	5	2	5	56.60	10.02
2	5	5	3	6	55.08	9.17
3	5	5	4	5.2	55/10	9.76
4	5	10	2	5.3	54.61	9.91
5	5	10	3	5.2	55.73	9.54
6	5	10	4	5.6	55.68	10.19
7	5	15	2	4.7	56.28	12.27
8	5	15	3	6.4	56.27	8.63
9	5	15	4	12.2	56.36	5.41
10	10	5	2	4.9	56.80	10.75
11	10	5	3	3	55.46	14.66
12	10	5	4	4.8	54.96	11/30
13	10	10	2	5.7	56.25	8.39
14	10	10	3	5.7	55.60	8.77
15	10	10	4	4.9	55/00	9.50
16	10	15	2	4.8	56.35	11.31
17	10	15	3	5.3	52.76	10.66
18	10	15	4	5.4	55.66	9.82
19	15	5	2	8.6	56.80	7.23
20	15	5	3	6	53.70	9.73
21	15	5	4	8	55.00	8.28
22	15	10	2	4.6	56.58	11.15
23	15	10	3	7.1	55.53	8.98
24	15	10	4	6.2	56.15	8.45
25	15	15	2	5.2	56.93	7.72
26	15	15	3	4.7	56.05	11.60
27	15	15	4	4.9	55.11	10.60

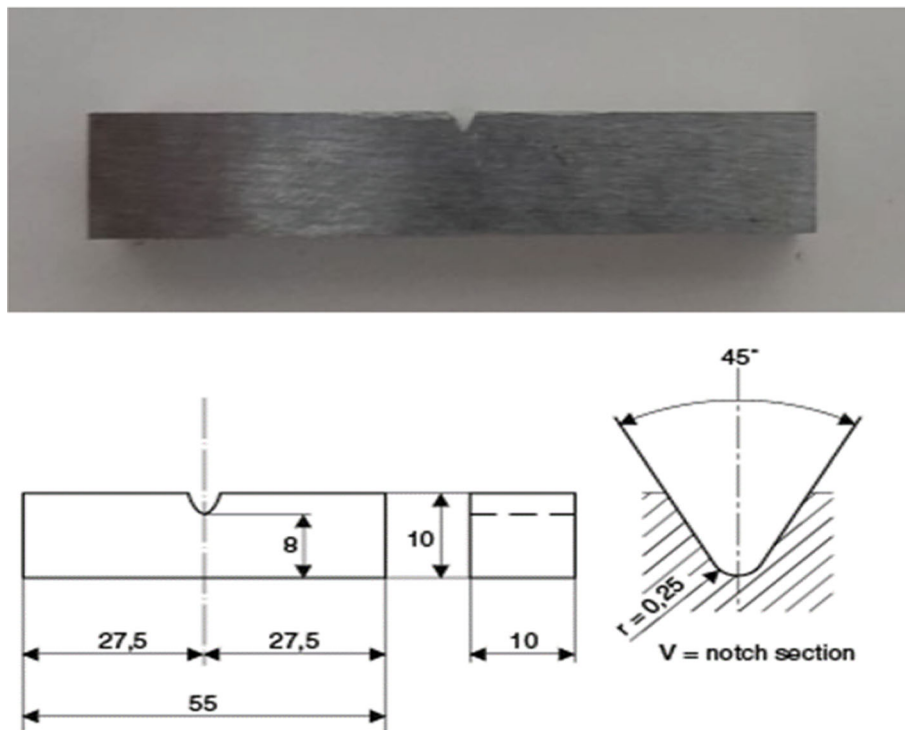


Fig. 3 Created V-shaped groove in the sample and the standard dimensions of the Charpy impact test

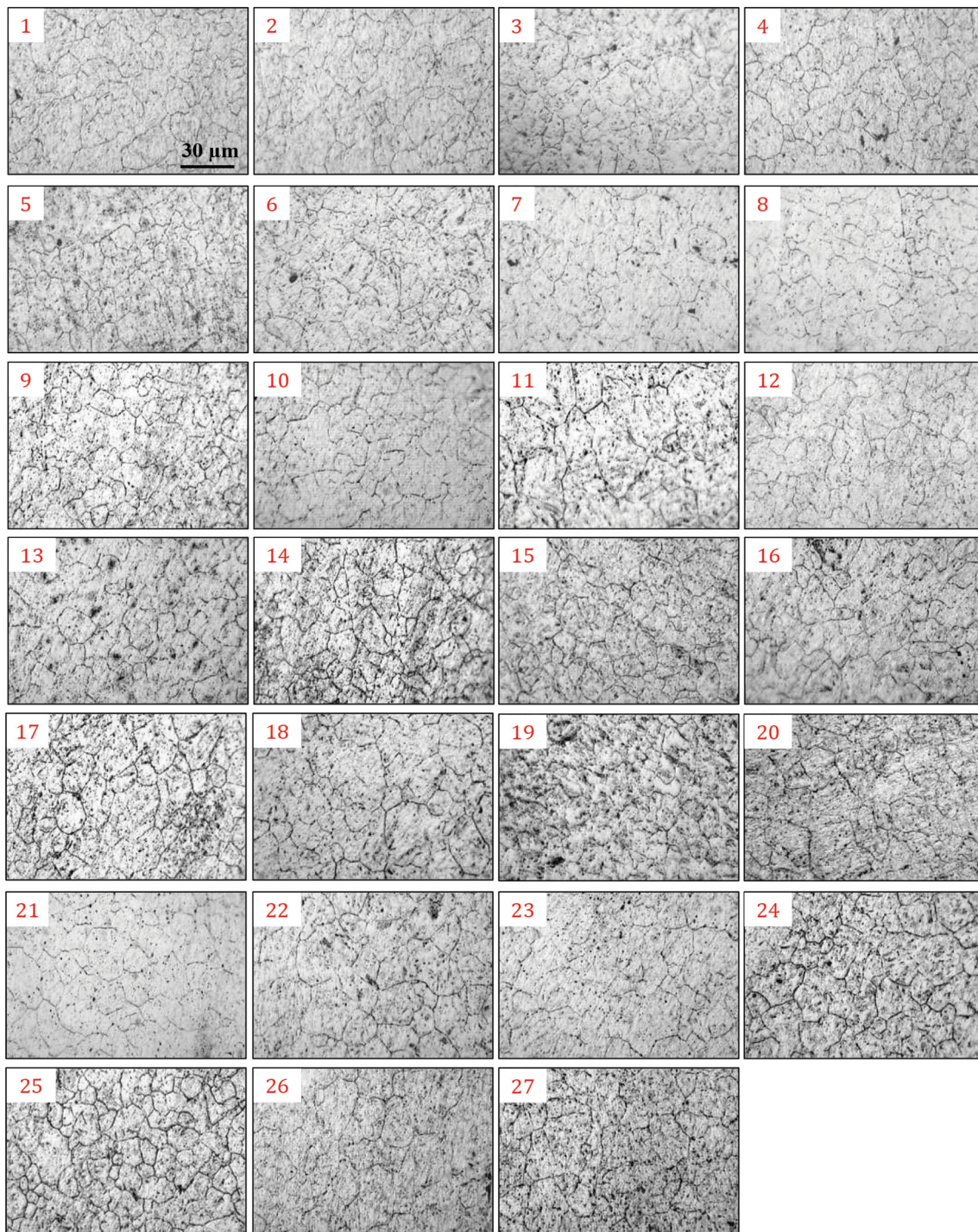


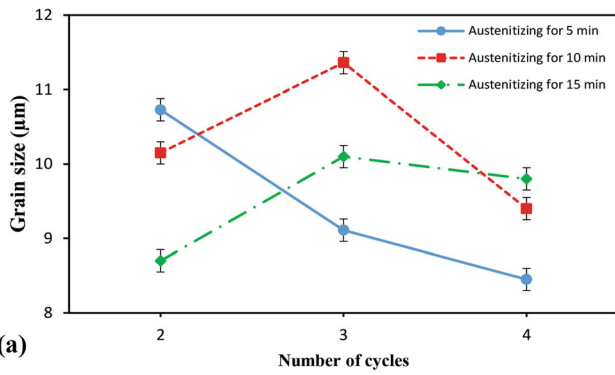
Fig. 4 OM images of 27 experiments (the scale of all images is the same)

are greatly influenced by these transformation temperatures. Figure 1 shows the CCT diagram for the steel used.

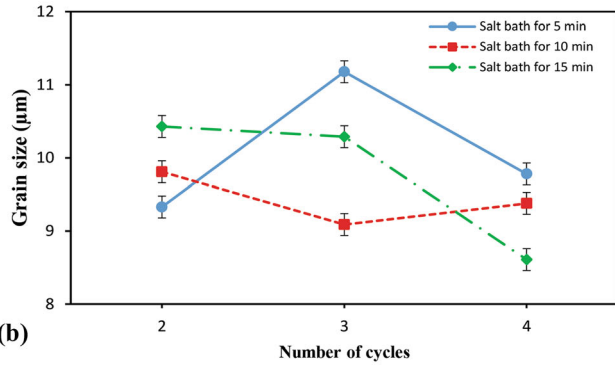
Figure 2 shows a schematic of the proposed cyclic heat treatment and the corresponding repetitive cycle. The first cycle (Fig. 2a) corresponds to the control sample (sample 0) and will be used to compare the results obtained. In this cycle, after the preheating process, the sample enters the austenitizing salt bath furnace and is kept for 15 min at 1040 °C. The sample is immediately quenched in the third furnace at 600 °C. After a

while, it becomes completely isothermal and cools slowly in the ambient air.

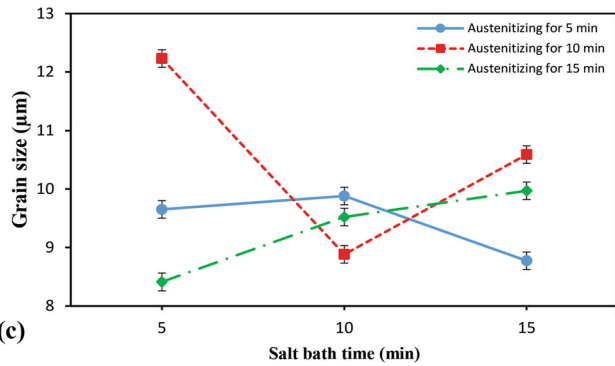
Figure 2(b) illustrates the diagram of cyclic heat treatment process for the other cycles. In the second cycle and after preheating, the sample is placed in an austenitizing salt bath furnace at 1040 °C and remains for a certain time. Then, it enters the second salt bath furnace at 750 °C and is kept for a certain time. Since the number of cycles is two, the sample repeats the same process once more, and finally, it is quenched in the third furnace at 600 °C. The sample is then slowly cooled



(a)

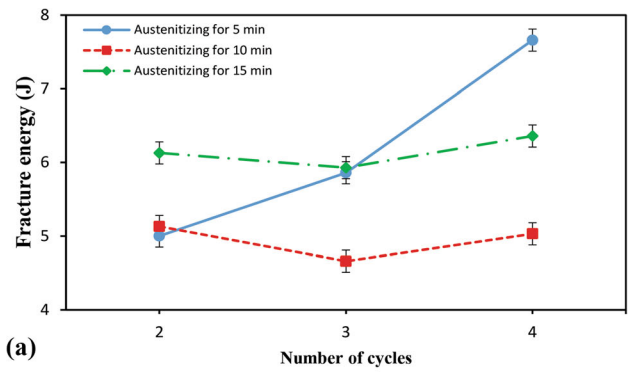


(b)

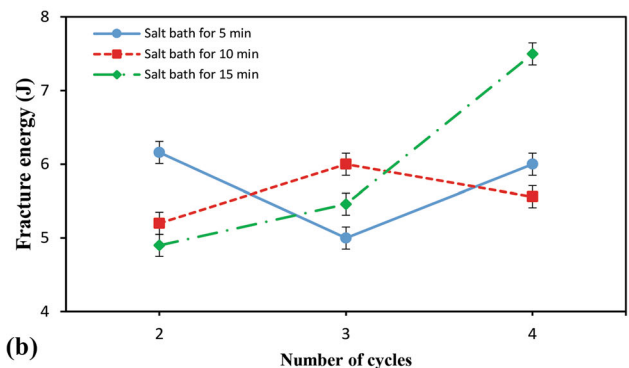


(c)

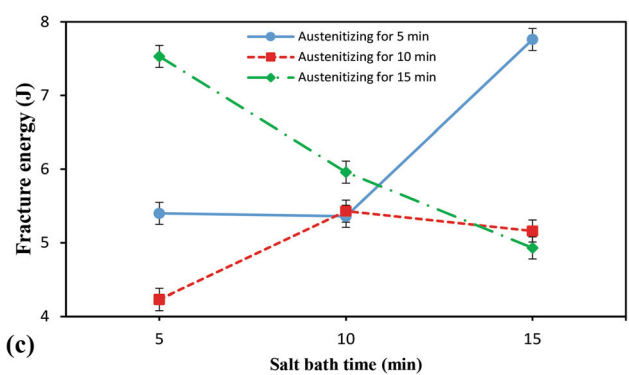
Fig. 5 Effect of austenitizing time, holding time in the intermediate bath and the number of cycles, on grain size



(a)



(b)



(c)

Fig. 6 Effect of austenitizing time, holding time in the intermediate bath and the number of cycles, on fracture energy

in the air. For the third and fourth cycles, the procedure described for the second cycle is repeated.

2.4 Design of Experiments

In this study, the full factorial design method was used to select the appropriate values of cyclic heat treatment parameters. Each of the three significant factors, including austenitizing time, holding time in the intermediate bath and number of cycles, were investigated at three levels. The total number of tests was 3^3 , and one sample was taken as a control test for comparison. Table 3 shows the design experiments with the MiniTab software. In both Table 3 and entire text, the term “grain size” refers to prior austenite grain size.

2.5 Evaluation Methods

Metallography, hardness measurement and Charpy impact test were performed after heat treatment. The samples were

polished and then etched with a solution of picric acid, penetrating solution and distilled water. The microstructure, prior austenite grain size, grain boundaries, fracture surfaces morphology, and phases present on the fracture surfaces were examined using a field emission scanning electron microscope (FESEM) model TESCAN-Mira III equipped with EDS analysis. The prior austenite grain size was determined manually using the linear intercept method by ImageJ software. Hardness is measured with a macro-hardness test by applying a load of 150 kgf for 15 s.

For the impact test, according to the ASTM A370 (Ref 18), a V-shaped groove with an angle of 45° , a depth of 2 mm and a root radius of 0.25 mm was created. This groove should not be created prior to heat treatment because thermal shocks will cause the sample to warp. Figure 3 shows images of the grooved specimen and the standard dimensions used in the Charpy impact test. A Charpy impact tester with a maximum power of 15 J and an accuracy of ± 1 J was used.

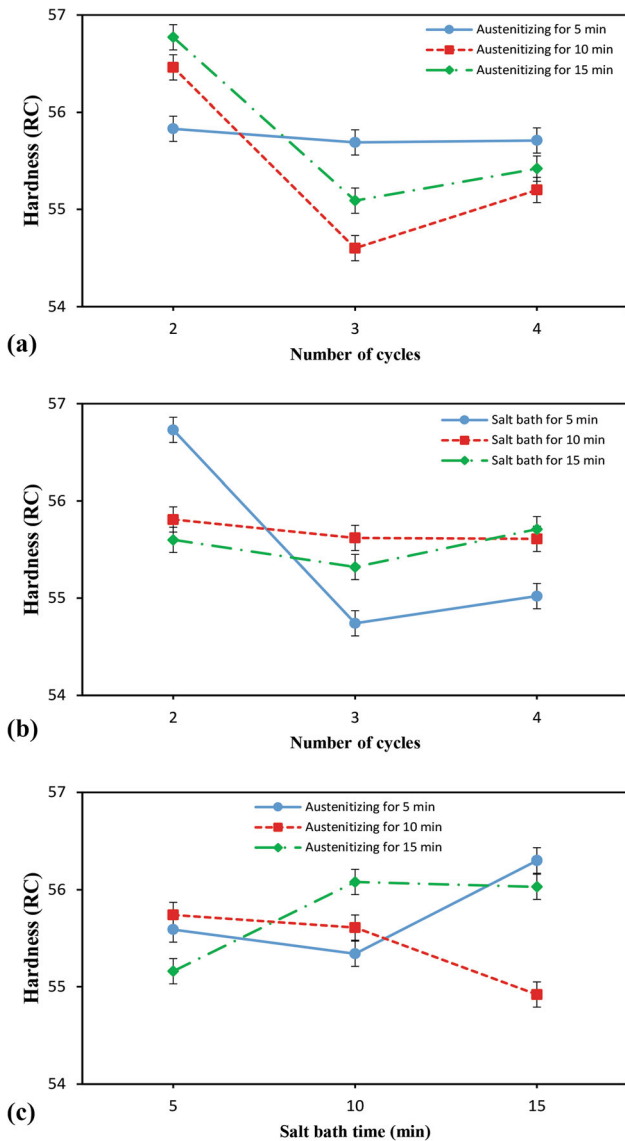


Fig. 7 Effect of austenitizing time, holding time in the intermediate bath and the number of cycles, on hardness

3. Results and Discussion

This work investigated the effect of variable parameters of cyclic heat treatment, including austenitizing time, holding time in the intermediate bath and number of cycles, on the microstructure and mechanical properties of AISI H13 hot work tool steel was investigated. Optical microscopy (OM) images for all 27 experiments are shown in Fig. 4. Grain boundaries of prior austenite are clearly visible in the microstructure. Quantitative values of grain size, hardness and fracture energy are given in Table 3.

The impact test results in Table 3 show that the highest toughness occurred in sample 9 with fracture energy of 12.2 J in 4 cycles. Also, the lowest toughness value was in sample 11 with fracture energy of 3 J in 3 cycles.

The sample's hardness before the tests was 20.87 RC (Rockwell C). Sample 25 has the highest hardness at heat treatment conditions of (15 min austenitizing time at 1040 °C, 15 min holding time at 750 °C and two cycles). For sample 25,

a fine-grained structure was obtained with a grain size of 7.7 μm . The lowest hardness was obtained in sample 17 in three cycles of heat treatment with an initial austenite grain size of 10.66 μm .

Examination of the prior austenite grain sizes in Table 3 shows that the smallest grain size is found in sample 9. The heat treatment conditions associated with this sample are: 5 min austenitization at 1040 °C, 15 min holding time at 750 °C in 4 cycles. This sample produced finer grains than all other samples. In addition, mechanical properties such as improved hardness and excellent toughness were observed in this sample. Sample 11 has the largest grain size and lowest toughness.

In summary, sample 9 has achieved an ultrafine structure with an average grain size of 5.41 μm , and a more uniform structure is observed compared to the other samples. The best mechanical properties, including excellent toughness and appropriate hardness, were achieved for this sample. In sample 11, the prior austenite grains are polyhedral and larger than the control sample. The average prior austenite grain size is 14.66 μm .

It can be concluded that the best toughness was obtained with a small grain size, which occurred under the following conditions: 5 min of austenitizing at 1040 °C, 15 min of holding at 750 °C in intermediate bath, and in 4 cycles. The lowest toughness was found in the sample with the largest grain size, which occurred after 10 min of austenitizing time, 5 min of intermediate salt bath time and 3 cycles. It was found that the grain size has a direct effect on impact energy values. In other words, as the grain size decreases, the impact strength increases, which is consistent with the results of previous research (Ref 19).

Figure 5 presents the effects of the number of heat treatment cycles, austenitizing times and holding time in the intermediate bath on grain size. In each of the graphs, the effect of the two parameters is examined by considering a fixed value for the third parameter. As can be seen in Fig. 5, the grain size decreased in two cycles with increasing austenitizing time (Fig. 5a) and decreasing holding time in the intermediate bath (Fig. 5b). At 4 cycles, the size of the prior austenite grains decreases by decreasing austenitizing time (Fig. 5a) and increasing the intermediate salt bath time (Fig. 5b). Contrary to the observations in two and four cycles, the grain size change does not show a progression as a function of the change in the austenitizing time and the holding time in the intermediate bath in three cycles. The smallest grain size occurred with the lowest austenitizing time and a moderate level of holding time in the intermediate bath. Assuming a constant heat treatment cycle, it can be seen from Fig. 5c that the grain size changes do not show any descriptive behavior in relation to the holding time in the intermediate bath and the austenitization time.

Figure 6 shows the effects of the number of cycles, austenitizing time and holding time in the intermediate bath on the fracture energy. During the two-cycle heat treatment, the fracture energy increases by increasing the austenitizing time (Fig. 6a) or decreasing the holding time in the intermediate bath (Fig. 6b). No consistent and descriptive behavior is observed in cycles 3 and 4. Figure 6(a) shows that the fracture energy increases with increasing number of cycles (at a constant level of holding time in the intermediate bath), but in general, this increase is not significant except for the austenitizing time of 5 min. The minimum fracture energy is recorded at the average level of the austenitizing time (10 min), but its value does not change significantly when the number of cycles changes.

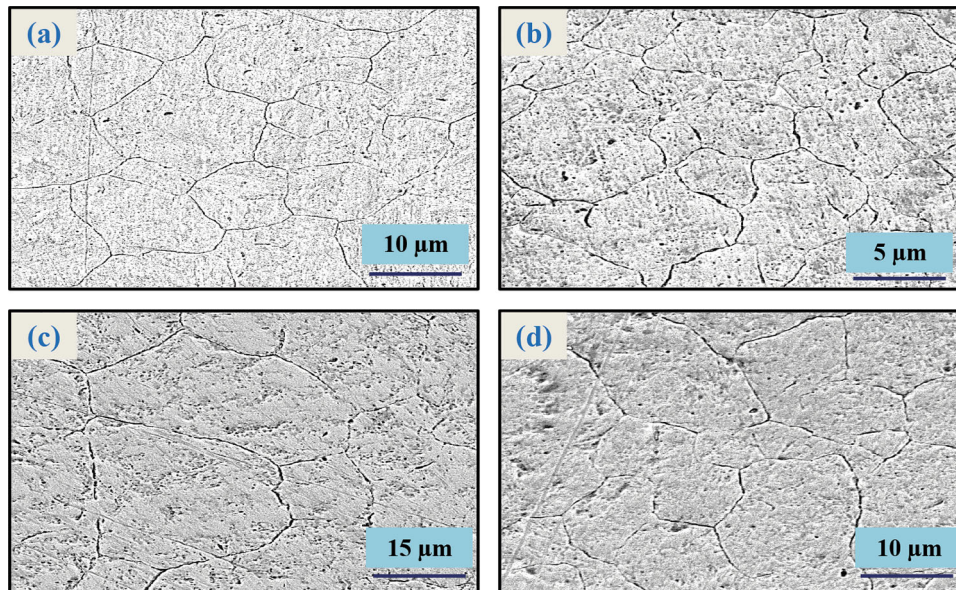


Fig. 8 FESEM images of (a) control sample, (b) sample 9, (c) sample 11 and (d) sample 18

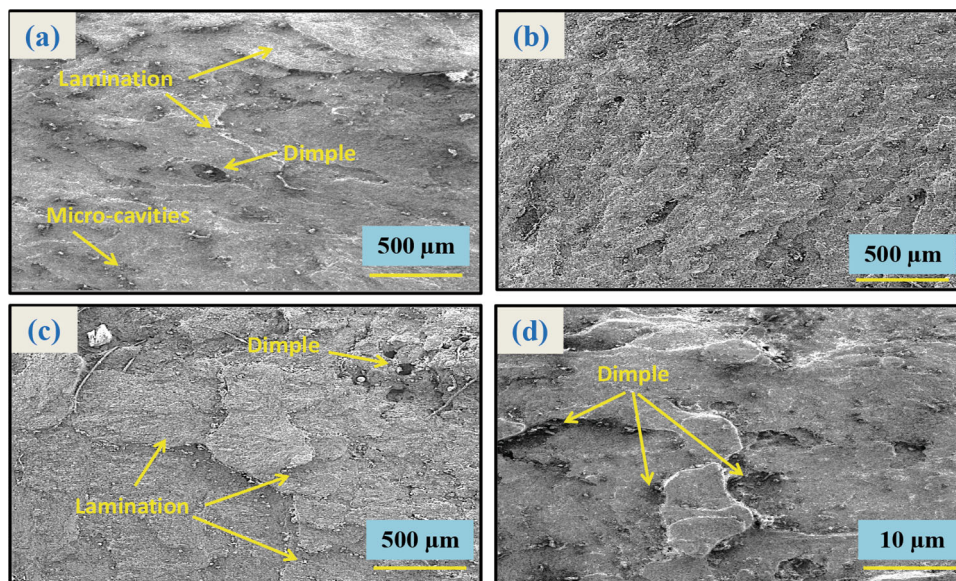


Fig. 9 Fracture surface morphology of (a) control sample, (b) sample 9, (c) sample 11 and (d) sample 18

Figure 6a shows that with the increase in the number of cycles, the fracture energy remains almost constant or increases in accordance with the austenitizing time. This observation can be somewhat generalized in Fig. 6(b). In general, it can be concluded that as the number of cycles increases, the fracture energy increases, and the sample becomes tougher. Figure 6(c) shows that the variation of the fracture energy with respect to the austenitizing time and holding time in the intermediate bath at a fixed number of cycles does not show a regular behavior that can be explained.

It is obvious from Fig. 7(a) and (b) that the highest hardness value was obtained in the sample with two heat treatment cycles. In two heat treatment cycles, increasing the austenitizing time and reducing the holding time in the intermediate bath increased the sample's hardness. Such behavior can be generalized to other cycles, but cannot be described as regular.

As shown in Fig. 7(c), the times of austenitizing and holding in the intermediate bath have little effect on the hardness of the sample.

To study the microstructure in different areas more fully and comprehensively, FESEM of control sample, sample 9, sample 11 and sample 18 is shown in Fig. 8. The selection of these samples is based on the prior austenite grain size results obtained in Table 3, which are related to the largest grain size (sample 11), the smallest grain size (sample 9), the average grain size (sample 18) and a control sample to compare the results .

In the FESEM image of the control sample in Fig. 8(a), the structure of prior austenite grains is multifaceted and grain boundaries are clearly visible. In sample 9 (Fig. 8b), grains with a size of approximately 5 μm were observed, which had a finer structure than the control sample and all other samples. This

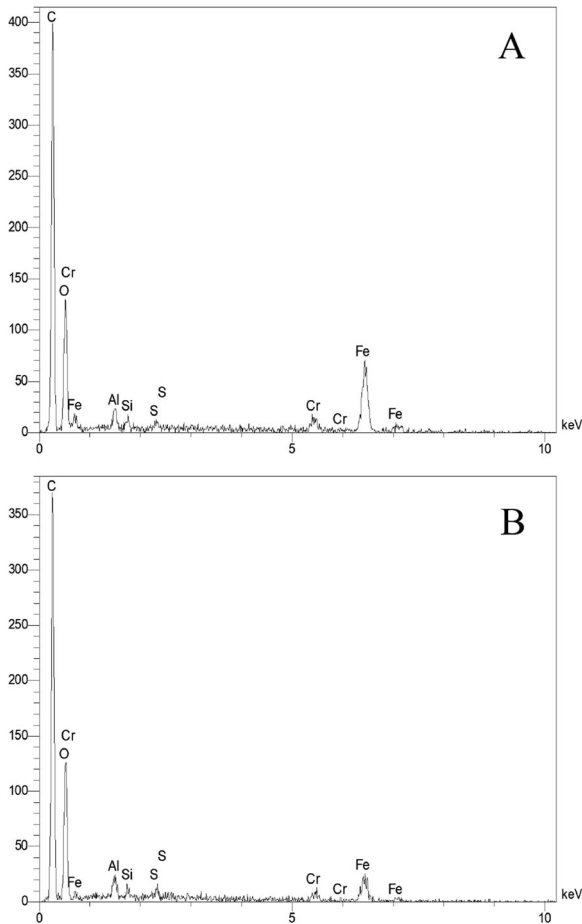
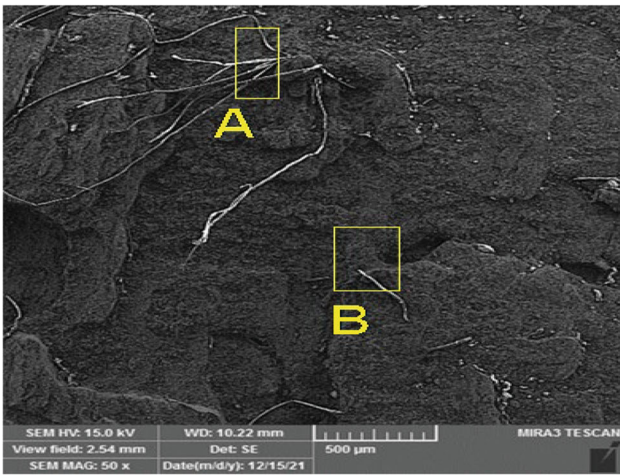


Fig. 10 EDX analysis of the fracture surface of sample 11 at points A and B

sample had good hardness and excellent toughness. In sample 11 (Fig. 8c), the initial austenite grain size was larger than that of the control sample, leading to a decrease in hardness and toughness. In sample 18 (Fig. 8d), the average prior austenite grain size was $9.8 \mu\text{m}$. The grain size is slightly different from the control sample and the hardness and toughness are almost equal to the control sample. A quantitative analysis reveals that sample 9, which has the smallest grain size, is approximately 63% finer than sample 11, which has the largest grain size. Additionally, when comparing sample 18, which has an average

grain size, to samples 9 and 11, there is a change of 44 and 33%, respectively. The results showed an increase in mechanical properties by decreasing the prior austenite grain size, which is consistent with previous studies. Also, by reducing prior austenite grain size of, toughness increases significantly.

The fracture surface morphology in different regions has been investigated for the 4 samples above and is shown in Fig. 9. The fractured surface of the sample has defects such as micro-cavities, lamination and dimples. The number of defects observed in sample 9 is very low (Fig. 9b). In sample 11, in addition to the micro-cavities and dimples present, more laminations were formed than in other samples (Fig. 9c). In sample 18, the number of dimples is large, and the lamination can be seen to some extent (Fig. 9d). As is known, many alloys fail by a mechanism known as the accumulation of very fine holes when they are subjected to continuous incremental loads. These holes are formed on the interface of the matrix phase with inclusions, secondary particles, grain boundaries or defects such as cracks and fine porosities. As the load increases, these micro-pores grow and coalesce, and eventually failure occurs. The size and number of dimples on the fracture surface depends on the number and distribution of micro-cavity nucleation sites. When the nucleation sites are small and far apart, the micro-cavities grow before coalescing, resulting in large dimples on the fracture surface. Therefore, when the number of micro-cavity nucleation sites is large, the size of dimples on the fracture surface is small, but their number is high (Ref 20).

Figure 10 presents the EDX analysis of sample 11 for further examination. The analysis shows that points A and B exhibit numerous elements, however, the amount of carbon present in these points surpasses that of the other elements. This finding confirms the precipitation of carbides at the grain boundaries of prior austenite, which makes the material more prone to intergranular brittle fracture. The formation of grain boundary carbides occurs during steel cooling after high-temperature austenitizing because more carbon is dissolved in austenite. Consequently, the primary cause of failure is brittle fracture due to carbide precipitation at the grain boundaries, leading to grain boundary fracture. The presence of grain boundary carbides increases the susceptibility to intergranular brittle fracture.

4. Conclusions

This research introduces a novel approach of cyclic heat treatment in a salt bath under A_{c1} temperature to attain an ultra-fine grain microstructure. The aim of this research was to assess how different cyclic heat treatment parameters affect the mechanical properties of AISI H13 hot work tool steel and to identify the optimal conditions for producing fine-grained microstructure. The austenitizing temperature of $1040 \text{ }^\circ\text{C}$, intermediate salt bath temperature of $750 \text{ }^\circ\text{C}$ and quenching salt bath temperature of $600 \text{ }^\circ\text{C}$ were kept constant, while the austenitizing times, holding times in intermediate bath and number of cycles were varied. The findings of the study demonstrated that:

- Optimal mechanical properties were achieved by subjecting the sample to 5 min of austenitizing process, followed by 15 min of intermediate salt bath and 4 cycles. This was further supported by the examination of the sample's microstructure, which revealed the least number of defects

compared to the other samples.

- By adjusting the austenitizing time and holding time in the intermediate bath, it is possible to achieve a fine-grained microstructure through numerous heat treatment cycles. Conversely, a fine-grained structure can also be attained with fewer cycles by increasing the austenitizing time and decreasing the holding time in the intermediate bath.
- The fracture energy of the sample was found to be significantly affected by an increase in the number of cycles. However, there was no observable impact on the fracture energy from changes in the austenitizing time or holding time in the intermediate bath.
- The fracture energy has been significantly improved without reducing or even increasing its hardness. Other methods of strengthening cannot achieve this level of improvement.
- The samples exhibited the greatest hardness when subjected to the fewest heat treatment cycles, while the duration of austenitizing and holding in the intermediate bath during a fixed number of cycles did not have a notable impact on the hardness.
- The main failure mechanism is brittle fracture due to carbide precipitation at the grain boundaries, leading to grain boundary fracture. The presence of grain boundary carbides increases the susceptibility to intergranular brittle fracture.

References

1. F. Deirmina, N. Peghini, B. AlMangour, D. Grzesiak, and M. Pellizzari, Heat Treatment and Properties of a Hot Work Tool Steel Fabricated by Additive Manufacturing, *Mater. Sci. Eng. A*, 2019, **753**, p 109–121
2. J.R. Davis, *ASM specialty handbook: tool materials*, ASM international, 1995
3. A. Persson, S. Hogmark, and J. Bergström, Simulation and Evaluation of Thermal Fatigue Cracking of Hot Work Tool Steels, *Int. J. Fatigue*, 2004, **26**, p 1095–1107
4. G. Telasang, J.D. Majumdar, G. Padmanabham, and I. Manna, Structure-Property Correlation in Laser Surface Treated AISI H13 Tool Steel for Improved Mechanical Properties, *Mater. Sci. Eng. A*, 2014, **599**, p 255–267
5. A. Saha, D.K. Mondal, and J. Maity, Effect of Cyclic Heat Treatment on Microstructure and Mechanical Properties of 0.6 wt% Carbon Steel, *Mater. Sci. Eng. A*, 2010, **527**, p 4001–4007
6. J. Dossett and G. Totten, *ASM Handbook, Volume 4D: heat treating of irons and steels*. ASM International, 2014
7. S. Maji, A.R. Subhani, B.K. Show, and J. Maity, Effect of Cooling Rate on Microstructure and Mechanical Properties of Eutectoid Steel Under Cyclic Heat Treatment, *J. Mater. Eng. Perform.*, 2017, **26**, p 3058–3070
8. J. Singh and S.K. Nath, Effects of Cyclic Heat Treatment on Microstructure and Mechanical Properties of 13%Cr-4%Ni Martensitic Stainless Steel, *J. Mater. Eng. Perform.*, 2020, **29**, p 2478–2490
9. V. Leskovšek, B. Šuštaršič, and G. Jutriša, The Influence of Austenitizing and Tempering Temperature on the Hardness and Fracture Toughness of Hot-Worked H11 Tool Steel, *J. Mater. Process. Technol.*, 2006, **178**, p 328–334
10. A. Chandan, G. Bansal, J. Kundu, J. Chakraborty, and S.G. Chowdhury, Effect of Prior Austenite Grain Size on the Evolution of Microstructure and Mechanical Properties of an Intercritically Annealed Medium Manganese Steel, *Mater. Sci. Eng. A*, 2019, **768**, 138458
11. H. Lan et al., Improvement of Strength-Toughness Combination in Austempered Low Carbon Bainitic Steel: The Key Role of Refining Prior Austenite Grain Size, *J. Alloy. Compd.*, 2017, **710**, p 702–710
12. B. AlMangour, D. Grzesiak, and J.-M. Yang, Nanocrystalline TiC-Reinforced H13 Steel Matrix Nanocomposites Fabricated by Selective Laser Melting, *Mater. Des.*, 2016, **96**, p 150–161
13. J. Wang, Z. Xu, and X. Lu, Effect of the Quenching and Tempering Temperatures on the Microstructure and Mechanical Properties of H13 Steel, *J. Mater. Eng. Perform.*, 2020, **29**, p 1849–1859
14. R. Ding et al., Failure Analysis of H13 Steel Die for High Pressure Die Casting Al Alloy, *Eng. Fail. Anal.*, 2021, **124**, 105330
15. F. Deirmina, B. AlMangour, D. Grzesiak, and M. Pellizzari, H13–Partially Stabilized Zirconia Nanocomposites Fabricated by High-Energy Mechanical Milling and Selective Laser Melting, *Mater. Des.*, 2018, **146**, p 286–297
16. J.-Y. Li, Y.-L. Chen, and J.-H. Huo, Mechanism of Improvement on Strength and Toughness of H13 Die Steel by Nitrogen, *Mater. Sci. Eng. A*, 2015, **640**, p 16–23
17. A.S.F. Testing and Materials, ASTM E23: Standard test methods for notched bar impact testing of metallic materials, 2012
18. I. ASTM, Standard test methods and definitions for mechanical testing of steel products. *ASTM A370*, 2012,
19. M. Koneshlou, K.M. Asl, and F. Khomamizadeh, Effect of Cryogenic Treatment on Microstructure, Mechanical and Wear Behaviors of AISI H13 Hot Work Tool Steel, *Cryogenics*, 2011, **51**, p 55–61
20. C.-P. Kang et al., Microstructure Evolution and Mechanical Properties of PESR 55Cr17Mo1VN Plastic Die Steel During Quenching and Tempering Treatment, *J. Iron. Steel Res. Int.*, 2021, **28**, p 1633

Publisher's Note Springer Nature remains neutral with regard to jurisdictional claims in published maps and institutional affiliations.

Springer Nature or its licensor (e.g. a society or other partner) holds exclusive rights to this article under a publishing agreement with the author(s) or other rightsholder(s); author self-archiving of the accepted manuscript version of this article is solely governed by the terms of such publishing agreement and applicable law.